Gene-expression profiling of systemic anaplastic large-cell lymphoma reveals differences based on ALK status and two distinct morphologic ALK$^+$ subtypes

Laurence Lamant,[1,2] Aurélien de Reyniès,[3] Marie-Michèle Duplantier,[1,2] David S. Rickman,[3] Frédérique Sabourdy,[1,2] Sylvie Giuriato,[1,2] Laurence Brugières,[4] Philippe Gaulard,[5] Estelle Espinos,[1,2] and Georges Delsol[1,2]

[1]Institut National de la Santé et de la Recherche Médicale (INSERM) U563 Centre de physiopathologie Toulouse Purpan, Toulouse, France; [2] Université Paul-Sabatier, Toulouse, France; [3]Programme Cartes d'Identité des Tumeurs (CIT), Ligue Nationale Contre le Cancer, Paris, France; [4] Department of Pediatric Oncology, Institut Gustave Roussy, Paris, France; [5]Department of Pathology, Inserm U 617, Hôpital Henri Mondor, Créteil, France

With the use of microarray gene-expression profiling, we analyzed a homogeneous series of 32 patients with systemic anaplastic large-cell lymphoma (ALCL) and 5 ALCL cell lines. Unsupervised analysis classified ALCL in 2 clusters, corresponding essentially to morphologic subgroups (ie, common type vs small cell and "mixed" variants) and clinical variables. Patients with a morphologic variant of ALCL had advanced-stage disease. This group included a significant number of patients who experienced early relapse. Supervised analysis showed that ALK$^+$ALCL and ALK$^-$ ALCL have different gene-expression profiles, further confirming that they are different entities. Among the most significantly differentially expressed genes between ALK$^+$ and ALK$^-$ samples, we found *BCL6*, *PTPN12*, *CEBPB*, and *SERPINA1* genes to be overexpressed in ALK$^+$ ALCL. This result was confirmed at the protein level for BCL-6, C/EBPβ and serpinA1 through tissue microarrays. The molecular signature of ALK$^-$ ALCL included overexpression of *CCR7*, *CNTFR*, *IL22*, and *IL21* genes but did not provide any obvious clues to the molecular mechanism underlying this tumor subtype. Once confirmed on a larger number of patients, the results of the present study could be used for clinical and therapeutic management of patients at the time of diagnosis. (Blood. 2007;109:2156-2164)

Introduction

Anaplastic large-cell lymphoma (ALCL) is considered a distinct entity in the World Health Organization (WHO) classification of lymphoid tumors.[1] Characteristically, 60% to 85% of these tumors express a chimeric protein, with transforming properties, in which the cytoplasmic portion of the anaplastic lymphoma kinase (ALK) tyrosine kinase is linked to a partner protein.[1,2] In most patients, ALK protein expression is attributed to the (2;5)(p23;q35) chromosome translocation, which fuses the *ALK* gene at 2p23 to the nucleophosmin *(NPM)* gene at 5q35.[3] However, several studies have shown that approximately one fifth of ALK$^+$ ALCLs are associated with other cytogenetic abnormalities in which the *ALK* gene at 2p23 is known to be fused to the *TPM3, TPM4, TFG, ATIC, CLTC, MSN, MYH9,* and *ALO17* genes.[4] All these translocations result in the expression of chimeric *ALK* transcripts that are translated into X-ALK fusion proteins, detectable by immunohistochemistry, with tyrosine kinase activity and oncogenic properties.

Although ALK$^+$ ALCL is considered a distinct entity, it shows a broad spectrum of morphologic features, some recognized in the WHO classification as common type, lymphohistiocytic, and small cell variants.[1] In addition, in some patients, different variants coexist in a single biopsy, and these tumors have been designated as mixed ALCL variants.[5] Another characteristic of these tumors is the perivascular pattern of neoplastic cells seen in a significant number of patients. The underlying biologic mechanism responsible for these strikingly different aspects is still unknown. Another controversy stems from the fact that some tumors (15%) with worse prognosis are morphologically and phenotypically similar to ALK$^+$ ALCL (ie, CD30$^+$, epithelial membrane antigen-positive [EMA$^+$], T-/null-cell phenotype) but are negative for ALK protein.[6] Finally, a significant proportion of patients with ALCL experience early relapses that are unpredictable and considered adverse prognostic factors.[7]

We undertook gene-expression profiling to identify whether distinct molecular signatures are associated with the presence and absence of ALK protein and with the various morphologic features. In this report, we show that ALK$^+$ tumors and ALK$^-$ ALCLs have different gene-expression profiles suggesting different oncogenic mechanisms associated with each type. In addition, we show that morphologic variants of ALCL—for instance, common type versus small cells and mixed variants—have distinct gene-expression signatures.

Patients, materials, and methods

Patients

The following frozen diagnostic tumor specimens from 32 patients with systemic ALCL were studied with patient informed consent: lymph node (29 patients), skin (2 patients), and soft tumor mass (1 patient). Histopathology and immunostaining results were reviewed independently by 3 hematopathologists (L.L., P.G., and G.D.). The percentage of malignant cells in each biopsy specimen was assessed using CD30 staining. Except for 4 patients (indicated by an asterisk in Figure 1), malignant cells accounted for at least 40% of the lymph node involvement. Diagnoses of ALCL were based on morphologic and immunophenotypic criteria, as described in the

Submitted June 13, 2006; accepted October 5, 2006. Prepublished online as *Blood* First Edition Paper, October 31, 2006; DOI 10.1182/blood-2006-06-028969.

The online version of this article contains a data supplement.

The publication costs of this article were defrayed in part by page charge payment. Therefore, and solely to indicate this fact, this article is hereby marked "advertisement" in accordance with 18 USC section 1734.

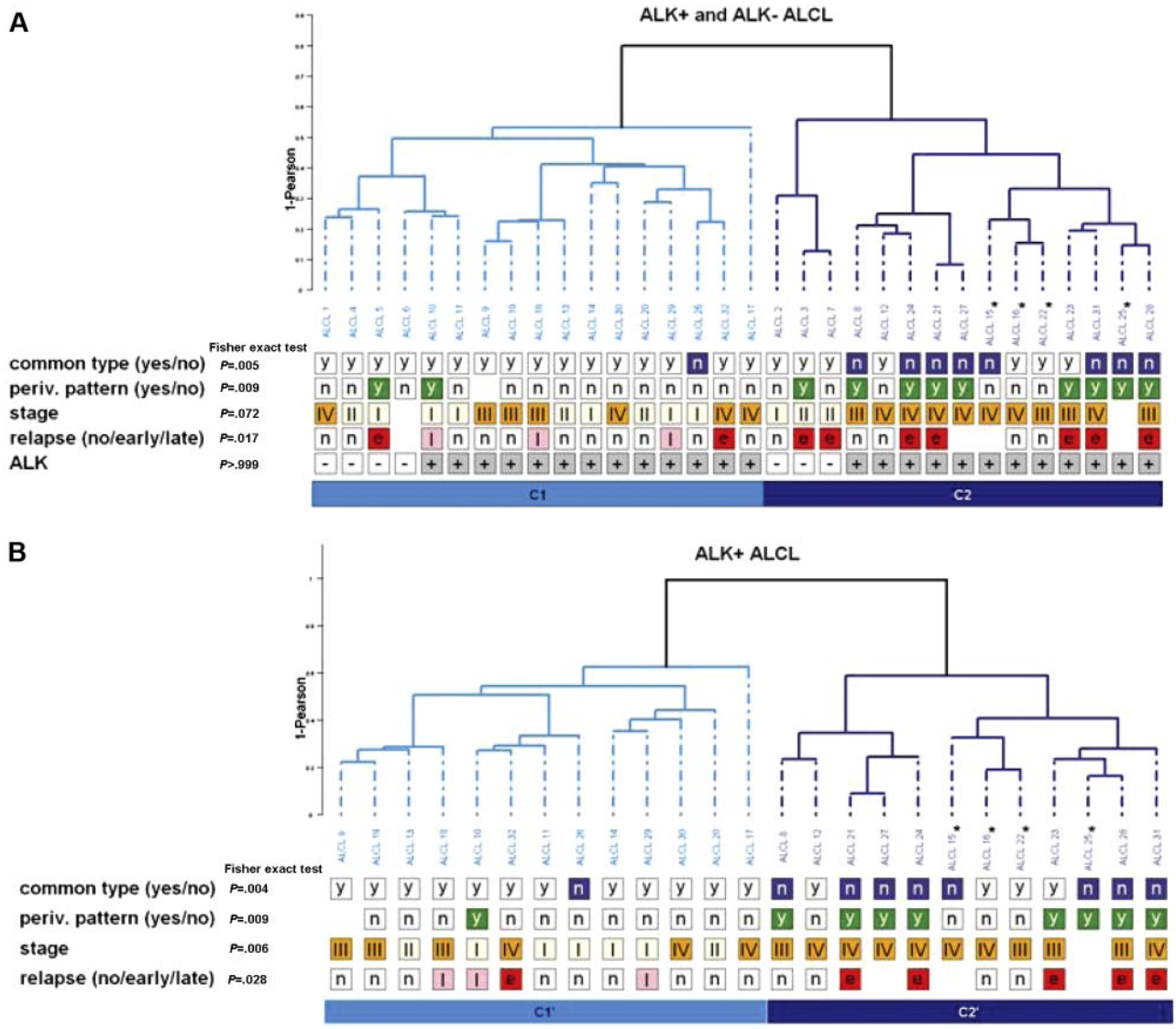

Figure 1. Pattern discovery. (A) Dendrogram. Hierarchical clustering of the 32 ALCL samples (ALK$^+$, 25; ALK$^-$, 7) based on 495 probe sets obtained by unsupervised selection (see "Patients, materials, and methods") using complete linkage. Common type (yes/no) corresponds to morphologic features: "y" denotes common type, and "n" denotes morphologic variants; periv. pattern (yes/no) corresponds to perivascular pattern: "y" denotes presence of malignant cells around vessels (see Figure 2D) and "n" denotes its absence; stage corresponds to Ann Arbor classification I, II, III, IV; relapse (no/early/late): n indicates no relapse; e, early relapse (delay less than 1 year); l, late relapse (delay more than 1 year); ALK corresponds to ALK1 immunostaining: minus = negative/plus = positive. Blanks denote "not available." Fisher exact test: *P* values measure association between each annotation and the partition C1/C2. Here, stage was recoded into a binomial variable: low, I-II; high, III-IV. Asterisks indicate the 4 patients with less than 40% of tumor cells: 10% (1 patient), 20% (2 patients), and 30% (1 patie, materials, nt). (B) Dendrogram. Hierarchical clustering of the 25 ALK$^+$ ALCL samples based on 198 probe sets obtained by unsupervised selection using complete linkage (see "Patients, materials, and methods"). Fisher exact test: *P* values measure association between each annotation and the partition C1′/C2′. Here, stage was recoded into a binomial variable: low, I-II; high, III-IV. Asterisks indicate the 4 patients with less than 40% of tumor cells, respectively 10% (1 patient), 20% (2 patients), and 30% (1 patient).

WHO classification.[1] All patients coexpressed CD30 and EMA, and most (29 of 32) had the T-cell phenotype, based on the expression of at least one T-cell–associated antigen (CD2, CD3, CD4, CD5, CD8, CD43). Most patients (n = 23) were also positive for cytotoxic associated antigen granzyme B and/or perforin. Twenty-three patients were classified with common type and 9 with morphologic (small cell or mixed) variants. In 11 tumors (4 common type and 7 morphologic variants), neoplastic cells showed a perivascular pattern. ALK expression was detectable in 25 patients using the ALK1 antibody. Staining was nuclear and cytoplasmic in 20 patients, suggesting a t(2;5)(p23;q35)/*NPM-ALK* translocation, and only cytoplasmic in the 5 remaining patients, with a membrane reinforcement in 3 patients, suggestive of a t(1;2)(q25;p23)/*TPM3-ALK* translocation. RT-PCR results were in perfect agreement with these staining patterns and demonstrated the expression of *TPM3-ALK* (3 patients), *MYH9-ALK* (1 patient), and *ATIC-ALK* (1 patient) transcripts in the 5 patients with restricted cytoplasmic ALK staining.[8-10] Because of the controversy regarding ALK$^-$ ALCL, only patients with tumors fulfilling strict morphologic and phenotypic criteria were included in the present study (ie, morphologic features consistent with common variant ALCL, coexpression of CD30 and EMA, and T-cell phenotype with the expression of perforin). Patients with primary cutaneous CD30$^+$ T-cell lymphoma and secondary ALK$^-$ ALCL were excluded.[1] Among the 32 patients, 19 were male and 13 were female (sex ratio, 1.46), median age at diagnosis was 16 years (range, 4-78 years), and median follow-up was 38.5 months (3.2 years). Eighteen patients had advanced stage III or IV disease at diagnosis, according to the Ann Arbor classification, and 12 patients had localized stage I or II disease. Disease stage in 2 patients, who died immediately after diagnosis, could not be determined. All patients but 2, who died before treatment, received multiagent chemotherapy, based on anthracycline and alkylant agents. Among these patients, 29 achieved complete remission and only one

achieved partial remission. Twelve patients experienced relapse/disease progression, and 9 of these relapses occurred within 12 months of diagnosis (5 children, 4 adults).

Twelve additional cases of systemic ALCL were retrieved from our tumor bank and used only for validation of Affymetrix results by quantitative RT-PCR (qRT-PCR). Approval for this retrospective study protocol was obtained from the CCPPRB (Comité Consultatif de Protection des Personnes dans la Recherche Biomédicale, Hôpitaux de Toulouse, France) Institutional Review Boards. Informed consent was provided in accordance with the Declaration of Helsinki.

Cell lines

Five ALCL cell lines were investigated, of which 4 were t(2;5)(p23;q35)–positive (Karpas 299,[11] SU-DHL-1,[12] COST,[13] PIO [our own laboratory unpublished cell line], and one ALK$^-$ [FE-PD]).[14] All of them were derived from common type ALCL[11,12] except for the COST cell line, established from a small cell variant ALCL.[13]

Microarray procedures

Samples were analyzed using Affymetrix GeneChip Human Genome U133A oligonucleotide arrays (http://www.affymetrix.com/support/index.affx). Total RNA was extracted from 40 frozen sections of tumor biopsies (each 5 μm thick) or from 1.0×10^7 cells, using the total SV RNA isolation kit (Promega, Charbonnières, France), which included a DNAse treatment to minimize genomic DNA contamination. RNA integrity and quantity were assessed on an Agilent 2100 Bioanalyzer (Agilent, Massy, France).

With the 1-cycle eukaryotic target labeling assay (Affymetrix, Santa Clara, CA), total RNA (5 μg) was first reverse transcribed using a T7-oligo(dT) promoter primer in the first-strand cDNA synthesis reaction. After RNase H-mediated second-strand cDNA synthesis, the double-stranded cDNA was purified and served as a template in the subsequent in vitro transcription (IVT) reaction. The IVT reaction was carried out in the presence of T7 RNA polymerase and a biotinylated nucleotide analog/ribonucleotide mix for complementary RNA (cRNA) amplification and biotin labeling. The biotinylated cRNA target was then purified, fragmented, and hybridized to an Affymetrix array. After overnight hybridization, arrays were incubated with phycoerythrin-conjugated streptavidin (SAPE) and biotinylated antibody against streptavidin and were scanned to obtain quantitative gene-expression levels.

Pattern discovery

Except when indicated, transcriptome analysis was carried out using either an assortment of R system software (version 1.9.0) packages including those of Bioconductor (version 1.1.1)[15] or original R code. Raw feature data from Affymetrix HG-U133A GeneChip microarrays were normalized using the robust multichip average (RMA) method[16] (package affy, version 1.4.32), which yielded $\log_2$ intensity expression summary values for each of the 22 283 probe sets. Probe sets corresponding to control genes or having an "_x_" annotation were masked, leaving 19 987 probe sets for further analysis.

Hierarchical clustering analysis of the 32 ALCL samples was derived from a series of 24 hierarchical cluster analyses, obtained from 8 data subsets and 3 different linkage methods (average, complete, and Ward), using 1-Pearson correlation as a distance metric (package class, version 7.2.2). Subsets of data corresponded to unsupervised selections of probe sets based on 2 criteria: minimal robust coefficient of variation (rCV) and maximal *P* value of a variance test (see "Variance test"). Between 98 and 5905 probe sets were selected (rCV thresholds spanning the 99.5th to the 60th percentiles and a *P* value lower than 0.01 for the test of variance). The intrinsic stability of initial dendrograms was assessed at a global level by comparing them with cluster results derived from perturbation/resampling tests (200 iterations for each). Perturbation of data sets was performed by the addition of random Gaussian noise ($\mu = 0$, $\sigma = 1.5 \times$ median variance calculated from the data set). We used the symmetric difference distance[17] as a stability measure. This distance is designed to compare 2 partitions and gives the proportion of retention of the pairs of samples that are in the same group (score is between 0 and 1: a score of 1 corresponds to equal partitions). Each dendrogram was cut to yield a partition of k groups (k = 2-8), and we compared partitions at each level of k. We also assessed the stability of the cluster groups obtained for each linkage from the 8 data subsets using the same stability measure. Moreover, for $k = 2$ groups, we identified consensus clusters, which are groups of samples that clustered together at least 95% of the time in the 24 dendrograms, each cut to yield 2 groups. One of the 24 dendrograms was selected for Figure 1A and the subsequent analyses because we found it to be representative of the segregation between common type ALCL and morphologic variant ALCL globally observed in the 24 dendrograms (see Table S5 [available at the *Blood* website; see the Supplemental Tables link at the top of the online article]). This dendrogram was obtained with the use of complete linkage on a subset of selected probe sets (n = 495), based on an rCV superior to the 97.5th rCV percentile and less than 10, and a *P* value of a variance test lower than 0.01.

Robust coefficient of variation. rCV for each probe set was calculated by dividing the standard deviation by the mean, eliminating the highest and lowest expression value across the samples for each probe set.

Variance test. We tested, for each probe set P, whether its variance was different from the median of the variances of the 19 987 probe sets. The statistic used was $[(n - 1) \times \mathrm{Var(P)}/\mathrm{Var_{med}})]$, where n refers to the number of samples. This statistic was compared to a percentile of the χ^2 distribution with $n - 1$ degrees of freedom and yielded a *P* value for each probe set. This criterion is used in the filtering tool of BRB ArrayTools software (version 3.2.0 beta 5; http://linus.nci.nih.gov/BRB-ArrayTools.html) and is described in the user's manual.

Association of ALCL subgroups and clinical/genetic variables

Fisher exact tests were carried out to determine the significance of the association between different clinical and genetic variables and the 2 ALCL tumor subgroups derived from each of the cluster analyses. For variables with multiple modalities (eg, stage), we also performed Fisher exact tests after a recoding into binomial values. Each combination was tested (eg, stage I vs II/III/IV; stages I/II vs III/IV). To adjust the association of a given variable to the 2 ALCL clusters for the effect of the other variables, we performed Mantel-Haenzel tests.

t Tests

We performed all univariate *t* tests using BRB ArrayTools software on the RMA normalized data. We selected probe sets having a *P* value below a given threshold (.001, except when indicated). To evaluate the number of false positives in this selection (because of multiple testing), we used a Monte-Carlo approach (implemented in BRB comparison tool[18]) based on 1000 random permutations of the label of the samples. Having ordered the list of probe sets by *P* value, this method evaluates the rank n for which the false discovery rate is lower than a chosen percentage (with a probability of 90%), where false discovery is relative to the chosen level of significance for the univariate test. This method also evaluates the rank n′, for which the number of false discoveries is less than a chosen number (with a probability of 90%).

Functional annotation using gene ontology

To assess the biologic functions and pathways associated with ALCL, we measured the underrepresentation and overrepresentation of gene ontology (GO) terms (association of gene products with regard to their associated biologic processes, cellular components, and molecular functions) in gene clusters derived from expression data with the use of FatiGO[19] and hypergeometric tests provided in the R package GOstats, version 1.1.1. We performed independent analyses of GO categories for overexpressed genes for C1′ relative to C2′ and C2′ relative to C1′. We performed tests on nonredundant lists of Entrez Gene identifiers (we used hgu133a meta-data library [version 1.7.0] to obtain Entrez Gene identifiers corresponding to a given list of probe sets).

Quantitative reverse transcription-PCR

cDNA were reverse transcribed from 2 μg total RNA, using Superscript II reverse transcriptase (Invitrogen, Cergy Pontoise, France) with oligo-dT as primers. Absence of genomic DNA contamination was checked by running RT-PCR with Raf8$^+$/raf9$^-$ primers, which hybridized on distinct exons spanning an intronic region. qRT-PCR was then performed on the cDNA diluted at 1:10 in sterile water, on an ABI7000 (Applied Biosystems, Courtaboeuf, France) with SYBR Green PCR reagents in a 25-μL reaction mixture (SYBR Green Jumpstart Taq Ready Mix; Sigma, Lyon, France). All primers were designed with Vector NTI advance 9.0 software (Invitrogen), and all spanned the region on the target gene covered by the corresponding Affymetrix probe set. Primers were used at a final concentration of 300 nM. Their sequences are listed in Table 1. All samples were run in duplicate. PCR was performed for 40 cycles at 95°C for 15 seconds and at 60°C for 1 minute after initial incubation at 50°C for 2 minutes and 95°C for 10 minutes. PCR product specificity was evaluated by generating a dissociation curve. The geometric mean Ct of *RPS3A, RPS18,* and *TBP* was used as a normalization factor to calculate ΔCt values [$\Delta Ct_{gene} = Ct_{gene} - \text{mean}(Ct_{RPS3A}, Ct_{RPS18}, Ct_{TBP})$].

Immunohistochemistry

Immunostaining was performed on paraffin sections of patients analyzed by Affymetrix arrays and additional patients included in an ALCL tissue microarray (TMA). Three antibodies were used: anti-C/EBPβ mAb (H7; Santa Cruz Biotechnology, Santa Cruz, CA), anti–BCL-6 mAb (code M7211; DakoCytomation, Trappes, France) and anti-serpinA1 polyclonal antibody (code A0012; DakoCytomation). Antibody binding was detected using the streptavidin-biotin-peroxidase complex (ABC) method and the Dako StreptABComplex/HRP Duet (mouse/rabbit) kit (code K492; DakoCytomation).

Results

Pattern discovery

Based on extensive cluster analysis using a series of the most varying genes across 32 samples (25 patients ALK$^+$ and 7 patients ALK$^-$) in combination with different linkage methods, we found a robust bipartition of the ALCL tumor samples. Figure 1A shows a dendrogram of the 32 ALCL samples using the top 2.5% most varying expression profiles (n = 495 probe sets; Table S1) and complete-linkage hierarchical clustering. Two distinct clusters were found, designated C1 and C2. ALK$^-$ patients clustered into 2 subbranches of the C1 and C2 groups (Figure 1A). Patients in cluster C1 primarily had ALCL with common type morphology (Figure 2A-B), whereas patients in group C2 primarily had morphologic variant ALCL ($P = .005$) (Figure 2C). In addition, the perivascular pattern of neoplastic cells was mostly found in the latter group ($P = .009$) (Figure 2D). When the same approach was applied to the 25 ALK$^+$ samples using the top 1% most varying expression profiles (n = 198 probe sets; Table S1), segregation of the samples into the same 2 clusters was strongly maintained because each of ALK$^+$ patients was assigned to the same cluster (now designated C1′ and C2′; Figure 1B). In addition to the differentiating morphologic features, patients in group C1′ had Ann Arbor stage I/II at diagnosis ($P = .006$), whereas those in group C2′ had advanced-stage disease (Ann Arbor III/IV). We found a significant number of patients in group C2′ who experienced early relapse (at most, 1 year after diagnosis; $P < .03$). Among the 841 probe sets (746 unique Entrez Gene identifiers; Table S2) differentially expressed between the C1′ and C2′ clusters, we found a statistically significant overrepresentation of genes involved in inflammatory and immune response, response to external stimulus, and stress response in the C1′ group. Moreover we found up-regulated genes involved in the leukocyte transendothelial migration pathway in the C1′ group, which is a key event in host defense, cytokine–cytokine receptor interaction, and natural killer cell–mediated cytotoxicity. On the other hand, genes overrepresented and up-regulated in the C2′ group were implicated in the regulation of the cell cycle and in cell proliferation. We also found the up-regulation of pathways such as purine and pyrimidine metabolism, glycolysis, and gluconeogenesis.

Table 1. Primers used for RT-qPCR

Gene name (affymetrix probe set)	Forward primer	Reverse primer
CEBPB (212501_at)	AAACTCTCTGCTTCTCCCTCTGC	CTGACAGTTACACGTGGGTTGC
CCR7 (206337_at)	AGACTTCTTGGCTTGGTGAGGA	AGGGGATGAGTGTGCTTTTAGG
MAC30 (212282_at)	GCCTCTACTTCCTCAGCCACAT	GCAGTGGGTCTTTGAACTCCTTA
GREM1 (218468_s_at)	TATGACTTTCTCTGAGTTGGGC	AAAGATTCAGGCACTGACTCAG
ALK (208212_s_at)	CCCACCTAACGTTGCAACTG	GCTGGTAGCCGTAATTGACA
TMOD1 (203661_s_at)	CAACGCAATGATGAACAACA	CATCCAGTTCAAAGGCATGG
RPS3A (201257_at)	CTTACCCGTGACAAAATGTGT	CGTATCTGATTGTTGCGTTT
RPS18 (201049_s_at)	CTGCAGCCATGTCTCTAGTGATC	CACCACATGAGCATATCTTCGG
TBP (203135_s_at)	ACCACAGCTCTTCCACTCACAG	AATCCCAGAACTCTCCGAAGCT
Raf8$^+$/raf9$^-$	GATGCAATTCGAAGTCACAGCG	TTTTCTCCTGGGTCCCAGATA

Molecular signature associated with ALK status in ALCL

To determine the most significant differentially expressed genes between ALK$^+$ ALCL and ALK$^-$ ALCL, 4 ALCL ALK$^+$ and 1 ALK$^-$ cell lines were included in the *t* test in addition to the 32 ALCL samples (25 patients with ALK$^+$, 7 patients with ALK$^-$), which gave more weight to genes expressed by the tumor cells. Among the list of 303 genes differentially expressed (Table S3), 117 genes were overexpressed in ALK$^+$ samples, and 186 were overexpressed in ALK$^-$ samples. Among the 117 genes overexpressed in patients with ALK$^+$ ALCL, several genes were highly statistically discriminatory between ALK$^+$ and ALK$^-$ samples ($P < .001$) (Table S3). The 4 top genes (excluding *ALK*) were *BCL6* (fold-change, 2.45), *PTPN12* (tyrosine phosphatase) (fold-change, 2.28), *CEBPB* (CCAAT/enhancer-binding protein β) (fold-change, 2.05), and *SERPINA1* (alpha-1 antitrypsin: *α1-AT* or *αPI*) (fold-change, 5.12).

The most significant overrepresented GO terms (biologic processes, cellular components, and molecular functions associated with gene products) in the ALK$^+$ group were related to immunologic functions (immune response, response to pathogen and parasite) and the I-κB kinase/NF-κB cascade.[20] Looking more specifically at the pathways associated with ALK$^+$ patients, we found an overrepresentation of pathways such as the leukocyte transendothelial migration *(ITGAM, PXN, JAM3)*, focal adhesion, and adherens junction *(CTNNB1/β-catenin, RAC1)*. In contrast, the functional categories of the genes overexpressed in ALK$^-$ ALCL did not provide any obvious clues to the molecular mechanism(s) underlying this tumor subtype because they tended to be associated

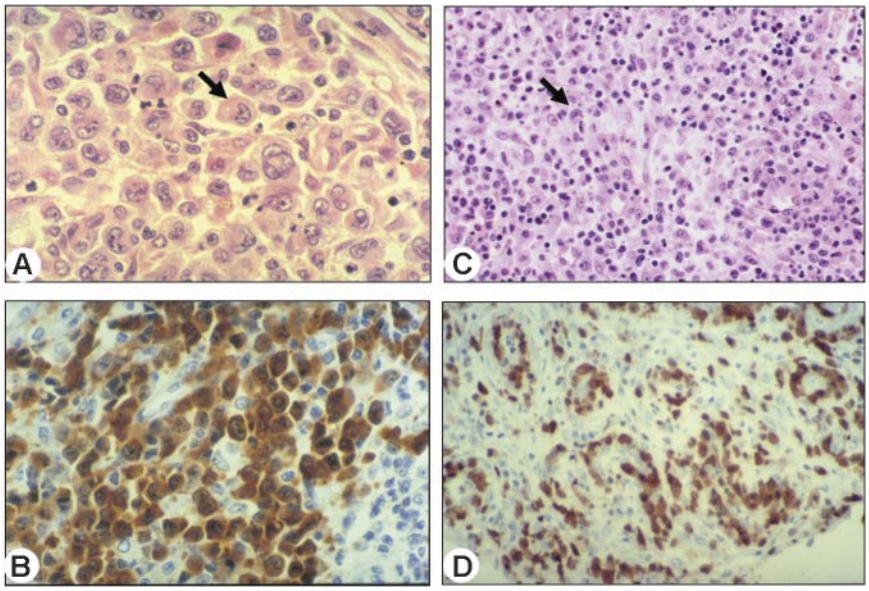

Figure 2. Morphologic variants and ALK staining illustrating 2 representative ALCL belonging to clusters C1 and C2, revealed by unsupervised analysis. (A) Common type ALCL (cluster C1) consists of large cells, including hallmark cells with a horseshoe shaped nucleus (arrow). Hematoxylin and eosin staining, magnified 1000 ×. (B) All malignant cells were strongly positive for ALK. Immunoperoxidase staining, magnified 1000 ×. (C) Small cell variant (cluster C2) with a predominant population of small cells with irregular nuclei, and scattered hallmark cells (arrow). Hematoxylin and eosin staining, magnified 400 ×. (D) Most of these cases are associated with a perivascular disposition of neoplastic cells highlighted by ALK staining. Immunoperoxidase staining, magnified 400 ×. Images were captured using a Leica DMR microscope equipped with an HC PL Fluotar 40×/0.85 numerical aperture (NA) or 100×/1.30 NA oil objective lens (Leica, Solms, Germany) and a Leica DFC 300 Fx camera. Images were processed using Leica IM50 image acquisition software.

with nonspecific biologic functions. We only found a statistically significant overrepresentation of genes up-regulated in these cases such as *CCR7, CNTFR, IL22,* and *IL21,* known to be involved in the cytokine–cytokine receptor interaction pathway.

Molecular signatures associated with morphologic features in ALCL

We found 491 probe sets corresponding to 447 genes that statistically differentiated common type ALCL and morphologic variants (only ALK^+ patients were considered because ALK^- [7 patients] was of common morphology) (Table S4). Of these, 248 genes were overexpressed in morphologic variants compared with common type ALCL, with a clear overrepresentation of 66 genes grouped together in the GO term cell communication. Most of these genes encode proteins involved in adhesion and migration, such as the focal adhesion kinase PYK2 (or PTK2B), a cytoplasmic tyrosine kinase of the FAK family. Genes coding for proteins that belonged to the focal adhesion complex and that played a critical role in the integrin-dependent cell motility—such as *PLCG2*, the catalytic subunits of the phosphoinositide 3-kinase (PIK3CA, PIK3CD) and several small G-proteins (ARHGDIB, GNB1, GRK5, RALB, RASSF2, RGS19, GNA13, CENTD2, DOK2, ARHGEF2, CENTA1, GPR18, ABR, RHOG)—were also overexpressed. We also found overexpression of the *SYK* gene encoding a tyrosine kinase protein, which becomes activated upon integrin-mediated adhesion and several genes encoding integrin-binding adhesion coreceptors, known to interact with these intracellular proteins, such as metalloproteases (ADAMTS2, ADAM12, ADAMDEC1) and molecules of the tetraspanin superfamily (CD37, CD53).

Confirmation of differential gene expression by qRT-PCR

To validate microarray experiment data, qRT-PCR was performed on 6 selected genes *(ALK, CEBPB, TMOD1, MAC30, CCR7, GREM1)*, in the list of differentially expressed genes between ALK^+ and ALK^- samples (Table S3). We selected these genes based on a prediction analysis of ALK status (data not shown). Three of them *(ALK, CEBPB, TMOD1)* were highly significantly differentially expressed between ALK^+ and ALK^- samples. Another 12 ALCL samples not analyzed with Affymetrix arrays were included in the analysis to test the validity of the results. Highly concordant results (median Pearson correlation coefficient between qRT-PCR and Affymetrix data, 0.86) were obtained for all 6 genes with statistically significant differences between ALK^+ and ALK^- tumors. Concordant results were also obtained by analyzing 10 randomly selected genes (data not shown).

Immunohistochemical validation of overexpressed genes using tissue microarrays

Among genes overexpressed in ALK^+ ALCL, we assessed the protein expression of C/EBPβ, BCL-6, and serpinA1. These proteins were chosen because corresponding antibodies suitable for use on tissue microarrays were commercially available. C/EBPβ expression was examined in 86 patients (65 ALK^+, 21 ALK^-), including 16 patients investigated with the use of Affymetrix. Strong nuclear staining for C/EBPβ was detected in 97% (63 of 65) of ALK^+ patients and in only 4.8% (1 of 21) of ALK^- patients (Figure 3). Forty (81.6%) of the 49 ALK^+ patients tested for BCL-6 showed a nuclear staining of neoplastic cells, whereas only 2 (28%) of the 7 ALK^- patients were positive ($P = .002$). Twenty-nine (78%) of the 37 ALK^+ patients were positively stained for serpinA1 whereas only 2 of the 9 ALK^- patients showed a cytoplasmic serpinA1 expression in tumor cells ($P < .003$).

Discussion

The recent development of DNA microarrays has provided new biologic insight into lymphoproliferative disorders. However, this approach has mainly been used for B-cell lymphomas, in particular diffuse large B-cell lymphoma,[21-24] primary cutaneous large B-cell lymphoma,[25] primary mediastinal B-cell lymphoma,[26] mantle-cell lymphoma,[27] B-cell chronic lymphocytic leukemia,[28] hairy-cell leukemia,[29] follicular lymphoma,[30] and multiple myeloma.[31] Using gene-expression profiling, some of these lymphoid neoplasms display a distinct molecular signature related to the cell of origin (eg, diffuse large B-cell lymphoma),[21,23] and in some tumors (eg, diffuse large B-cell lymphoma and follicular lymphoma),[23,30] it is even possible to predict outcome on the basis of individual genes expressed by nonneoplastic infiltrating cells. By contrast, few studies have been dedicated to peripheral T-cell lymphomas.[32-35]

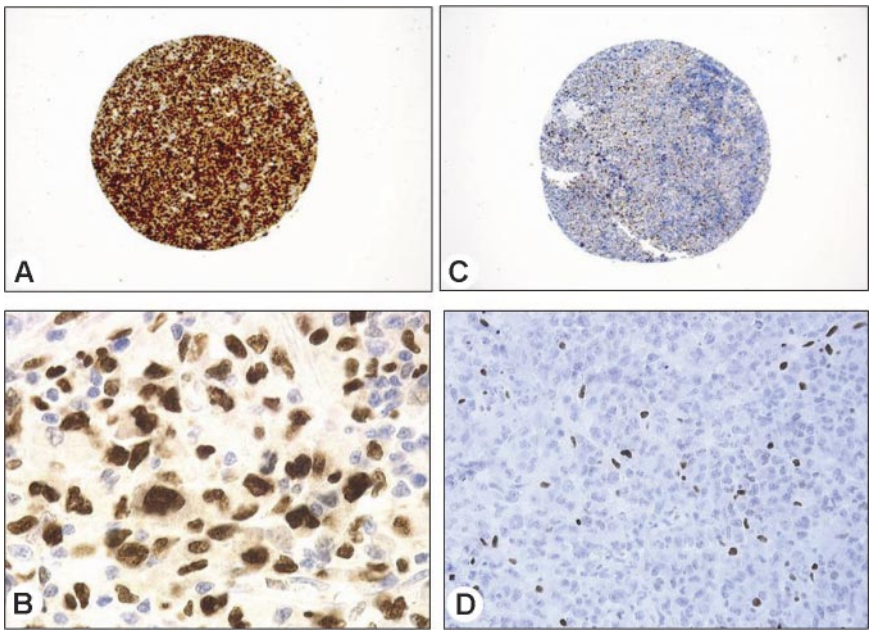

Figure 3. Immunohistochemical validation of some overexpressed genes using tissue microarrays. Immunostaining of 2 representative cases of ALK$^+$ (A-B) and ALK$^-$ (C-D) ALCL. Malignant cells in the ALK$^+$ patient strongly express C/EBPβ (A-B). Immunoperoxidase staining, magnified 50 × and 1000 ×. In the patient negative for ALK protein, only reactive histiocytes show strong nuclear staining (C-D). Immunoperoxidase staining, magnified 50 × and 400 ×. Images were captured and processed as described in Figure 2, except that an HC PL Fluotar 5×/0.15 NA objective was used for panels A and C.

T-cell lymphomas represent a heterogeneous group of tumors that could benefit from DNA microarrays for defining unrecognized subcategories, identifying new oncogenic pathways or pathogenetically relevant genes and biologic predictors for their clinical course. With the exception of previous reports based on cell lines derived from T-cell malignancies,[36-38] few studies involve biopsy specimens from patients with T-cell lymphomas.[32-35] In the study by Martinez-Delgado et al,[32] gene-expression profiles have been analyzed in 34 peripheral T-cell lymphoma pertaining to different categories. They found only 35 genes distinguishing all peripheral T-cell lymphomas from reactive lymph nodes, but they were unable to establish the molecular signature of each category. The latter series included only 5 patients with systemic ALCL.

Our study is the first report using oligonucleotide microarray gene-expression profiling in a homogeneous series of 32 patients (25 ALK$^+$, 7 ALK$^-$) with systemic ALCL. In contrast to Thompson et al,[33] only systemic ALK$^-$ ALCL fulfilling strict criteria were included in the present study (see "Patients, materials, and methods"). The main goal of the present study was to address 2 major open questions regarding ALCL. First, do ALK$^+$ and ALK$^-$ ALCL tumors have different gene-expression profiles, suggesting that they are different entities involving distinct oncogenic mechanisms? Second, are the various morphologic features of ALCL (eg, common type vs morphologic variants) merely morphologic variations of the same disease entity with a single molecular signature or are they associated with different gene profiling expression?

Although primary systemic ALK$^+$ ALCL is a well-defined entity in the WHO classification, so-called ALK$^-$ ALCL is still the subject of controversy. In our unsupervised analysis (Figure 1A), ALK$^-$ patients clustered into 2 subbranches in C1 and C2, further suggesting that ALK$^-$ ALCL is heterogeneous and belongs to entities different from those for ALK$^+$ ALCL. These results are in agreement with the recent study by Ballester et al[34] showing a clear segregation between ALK$^+$ and ALK$^-$ patients by using hierarchical clustering analysis of T-cell non-Hodgkin lymphomas. In the present study, the supervised analysis by class comparison between ALK$^+$ and ALK$^-$ ALCL tumors provided distinct molecular signatures. The molecular signature of ALK$^-$ ALCL includes overexpression of 4 genes with the most significant *P* value—*CCR7, CNTFR, IL22,* and *IL21*—but did not allow identification of the underlying oncogenic mechanism associated with these tumors. Among the genes overexpressed in ALK$^+$ ALCL, *BCL6, PTPN12, SERPINA1,* and *CEBPB* are the 4 top genes overexpressed with the most significant *P* value.

Overexpression of the *BCL6* proto-oncogene in ALK$^+$ ALCL was confirmed by immunohistochemistry. These results are in agreement with previous reports, although the percentage of positive cases (approximately 40% in previous studies, including ALK$^+$ and ALK$^-$ patients) was lower than in our study (overall, 75% of all patients).[39,40] Such a discrepancy could be explained by the overrepresentation of ALK$^+$ patients in our series. BCL-6 is known to be predominantly expressed in germinal center B lymphocytes and their neoplastic counterparts,[41] and there is no clear explanation concerning its expression in T-/null-cell ALCL.[39] However, BCL-6 is also expressed by a subpopulation of germinal center and perifollicular CD4$^+$ T lymphocytes and by a small population of CD30$^+$ cells localized in the perifollicular area and at the edge of germinal centers.[39,42] These CD4$^+$/BCL-6$^+$ T cells might correspond to the recently described follicular B-helper T cells (T_{FH}),[43] but the latter cells are characteristically positive for CXCL13, a chemokine that is exceptionally expressed in ALCL[44] and, in contrast to CXCL12, not found in the present study. Moreover, BCL-6 overexpression in ALK$^+$ ALCL is in agreement with the down-regulation of the cyclin D2 gene, also found in these tumors (data not shown) because the latter gene is known to be negatively regulated by BCL-6.[45]

PTPN12 (also named *PTP-PEST*) was the second statistically discriminatory gene overexpressed in ALK$^+$ samples. The expression of this tyrosine phosphatase, originally cloned from a human colon cancer cDNA library,[46] has never been reported in lymphoma. This phosphatase has been described as a negative regulator of c-abl kinase activity.[47] We should note that we have recently shown that SHP1, another protein tyrosine phosphatase, is also expressed in ALK$^+$ ALCL and involved in NPM-ALK dephosphorylation.[48]

A potentially interesting gene overexpressed in ALK$^+$ ALCL is the SERPINA1 gene. SerpinA1 is a major plasma serine proteinase inhibitor that is mostly synthesized by the liver but is also

synthesized by a number of other cells, including monocytes/macrophages.[49] On the basis of morphologic ground and serpinA1 expression, some hematopoietic neoplasms were originally diagnosed as malignant histiocytosis or true histiocytic lymphoma and were later reclassified as ALCL.[50,51] The overexpression of serpinA1 in ALK$^+$ ALCL is in agreement with the results reported by Villalva et al[52] using subtractive suppressive hybridization technique between an ALK$^+$ ALCL cell line and an ALK$^-$ ALCL tumor. Of note, increased serpinA1 levels in sera or tumor tissues from various cancer patients have been reported.[53,54] Interestingly, in these studies, patients with tumors positive for serpinA1 had worse prognoses than those with negative ones. The adverse prognostic effect of serpinA1 expression could be related to its inhibition of natural killer (NK)–cell activity.[55-57]

CEBPB is the fourth gene that discriminated ALK$^+$ and ALK$^-$ samples and was highly correlated with ALK expression. Overexpression of C/EBPβ in ALK$^+$ tumors was confirmed by immunohistochemistry. Recently, Jundt et al[58] demonstrated in ALCL cell lines that the overexpression of C/EBPβ, via the Akt/mTOR (mammalian target of rapamycin) pathway activation, led to increased cell proliferation. A body of evidence suggests that C/EBPβ proteins play a central role in the balance between cell differentiation and proliferation.[59] This dual activity is based on the ratio between the main isoforms (LAP and LIP) transcribed from a single mRNA. Full-length LAP (liver-enriched activating protein) drives the cell to the differentiation pathway and cycle arrest, whereas the truncated isoform LIP (liver-enriched inhibitory protein) promotes cell proliferation.[60] Because of the lack of specific anti-LIP antibody, we could not determine the expression of the C/EBPβ LIP isoform through immunohistochemistry in biopsy specimens. Given that expression of the LIP isoform of C/EBPβ was based on activation of the Akt/mTOR pathway,[58] in the absence of available specific ALK inhibitors, therapeutic drugs such as rapamycin targeting this pathway could be envisaged.

The ALK$^+$ signature also included genes implicated in the leukocyte transendothelial migration pathway and adherens junction pathway. Most of the latter genes are involved in the Wnt signaling pathway such as *CTNNB1*/β-catenin, frequently deregulated in a number of human malignancies,[61-63] and *RAC1*.[64] It has been demonstrated that in the presence of Wnt, CTNNB1/β-catenin is stabilized and translocated to the nucleus, where it associates with members of the TCF/LEF family of transcription factors, such as TCF4.[65] Interestingly, in ALK$^+$ ALCL we found an overexpression of TCF4 (3-fold average change), which could account for the overexpression of the Wnt target gene *FOSL1* (fos-like antigen or *fra-1*, 2-fold average change).[66] The deregulation of the β-*catenin* gene expression could lead to the loss of cell-cell adhesions[61] and might explain the frequent extranodal involvement in ALK$^+$ patients.[1]

Another aim of the present study was to determine whether the various morphologic features of ALCL (common type vs small cell/lymphohistiocytic variants) are merely morphologic variations of the same disease entity and share the same molecular signature or whether they are associated with a distinct gene profile.[1] It could be anticipated that the gene-expression profiles of these 2 groups (common type vs morphologic variants) would be different. Using cluster analysis based on the most varying genes across our series of ALK$^+$ samples, we found a robust bipartition of the ALCL tumor samples. One cluster (C1′) consisted mainly of common type ALCL, whereas morphologic variants clustered in the other group (C2′), where tumors showing a perivascular disposition of neoplastic cells were also found. Such a clustering may appear to be at odds with previous studies, suggesting that these morphologic variants are variations of a single disease entity.[5] Most important, a significant number of patients in group C2′ experienced early relapse (at most, 1 year after diagnosis; $P < .03$). Among the genes differentially expressed between the C1′ and C2′ clusters, we found a statistically significant overrepresentation of genes involved in inflammatory and immune response, response to external stimulus, and stress response in the C1′ group. Moreover, in the latter group, we found a clear overrepresentation of genes encoding proteins involved in adhesion and migration, particularly in focal adhesion complexes such as PYK2, PLCγ2, PIK3CA, PIK3CD, and several small G-proteins. On the other hand, genes overrepresented and up-regulated in the C2′ group were implicated in the regulation of the cell cycle and in cell proliferation. We also found the up-regulation of pathways, such as purine and pyrimidine metabolism, glycolysis, and gluconeogenesis, that could reflect the cellular hyperactive status. To reconcile the concept of a unique entity and the finding of the 2 gene-expression profiles found in clusters C1′ and C2′, we postulate that in the course of the disease, some patients may switch on or switch off a set of genes, resulting in different morphologic features.

In summary, with the use of gene-expression profiling, we show that ALK$^+$ and ALK$^-$ ALCLs have different gene-expression profiles, further confirming that they are different entities. In addition, preliminary results of the present study may have clinical implications because they suggest that tumors in patients who experience relapse within 1 year of diagnosis express a set of genes that, if confirmed on a larger number of patients, could be of clinical and therapeutic value.

Acknowledgments

This work was supported by the Ligue Contre le Cancer, Comités de la Haute-Garonne et de l'Aveyron, and the program Carte d'Identité des Tumeurs, Fondation de France, Cancéropôle Grand Sud-Ouest: projet cibles thérapeutiques dans les hémopathies malignes, Conseil Régional Midi-Pyrénées and Contrat Interface INSERM-CHU Purpan (Toulouse, France) (L.L.).

We thank Michel March for his excellent technical work performing immunohistochemistry. We also thank Nicole Dastugue for assistance with cytogenetic work and Fabien Petel (Ligue Nationale Contre le Cancer) for his help formatting the data to be MIAME compliant and submitting the data to the EBI. We thank the Société Française des Cancers de l'Enfant and the Groupe d'Etude des Lymphomes de l'Adulte for providing clinical annotations. We thank our fellow pathologists Dr Fanny Gaillard (CHU de Nantes) and Dr Frédérique Dijoud (CHU de Lyon) for providing frozen samples.

Authorship

Contribution: L.L., E.E., and G.D. designed the research. M.-M.D., F.S., and S.G. performed the research. L.B. and P.G. collected the data. A.d.R., D.S.R., E.E., and L.L. analyzed the data. A.d.R. and D.S.R. contributed vital analytical tools. L.L., E.E., G.D., A.d.R., and D.S.R. wrote the paper.

Conflict-of-interest disclosure: The authors declare no competing financial interests.

L.L. and A.d.R. contributed equally to this work. E.E. and G.D. are senior coauthors.

Correspondence: Georges Delsol, Centre de Physiopathologie Toulouse-Purpan, Inserm U-563, Bât. B, CHU-Purpan, Place du Docteur Baylac, BP 3028, 31024 Toulouse Cedex 3, France; e-mail: gdelsol@toulouse.inserm.fr.

References

1. Delsol G, Ralfkiaer E, Stein H, Wright D, Jaffe ES. Anaplastic large cell lymphoma: primary systemic (T/null cell type). In: Jaffe ES, Harris NL, Stein H, eds. World Health Organization (WHO) Classification of Tumours: Pathology and Genetics of Tumours of Haematopoietic and Lymphoid Tissues. Lyon, France: IARC Press; 2001:230-235.
2. Stein H, Foss HD, Durkop H, et al. CD30(+) anaplastic large cell lymphoma: a review of its histopathologic, genetic, and clinical features. Blood. 2000;96:3681-3695.
3. Morris SW, Kirstein MN, Valentine MB, et al. Fusion of a kinase gene, ALK, to a nucleolar protein gene, NPM, in non-Hodgkin's lymphoma. Science. 1994;263:1281-1284.
4. Pulford K, Lamant L, Espinos E, et al. The emerging normal and disease-related roles of anaplastic lymphoma kinase. Cell Mol Life Sci. 2004;61:2939-2953.
5. Benharroch D, Meguerian-Bedoyan Z, Lamant L, et al. ALK-positive lymphoma: a single disease with a broad spectrum of morphology. Blood. 1998;91:2076-2084.
6. Gascoyne RD, Aoun P, Wu D, et al. Prognostic significance of anaplastic lymphoma kinase (ALK) protein expression in adults with anaplastic large cell lymphoma. Blood. 1999;93:3913-3921.
7. Brugieres L, Deley MC, Pacquement H, et al. CD30(+) anaplastic large-cell lymphoma in children: analysis of 82 patients enrolled in two consecutive studies of the French Society of Pediatric Oncology. Blood. 1998;92:3591-3598.
8. Colleoni GW, Bridge JA, Garicochea B, Liu J, Filippa DA, Ladanyi M. ATIC-ALK: a novel variant ALK gene fusion in anaplastic large cell lymphoma resulting from the recurrent cryptic chromosomal inversion, inv(2)(p23q35). Am J Pathol. 2000;156:781-789.
9. Lamant L, Dastugue N, Pulford K, Delsol G, Mariame B. A new fusion gene TPM3-ALK in anaplastic large cell lymphoma created by a (1;2)(q25;p23) translocation. Blood. 1999;93:3088-3095.
10. Lamant L, Gascoyne RD, Duplantier MM, et al. Non-muscle myosin heavy chain (MYH9): a new partner fused to ALK in anaplastic large cell lymphoma. Genes Chromosomes Cancer. 2003;37:427-432.
11. Fischer P, Nacheva E, Mason DY, et al. A Ki-1 (CD30)-positive human cell line (Karpas 299) established from a high-grade non-Hodgkin's lymphoma, showing a 2;5 translocation and rearrangement of the T-cell receptor beta-chain gene. Blood. 1988;72:234-240.
12. Epstein AL, Kaplan HS. Biology of the human malignant lymphomas, I: establishment in continuous cell culture and heterotransplantation of diffuse histiocytic lymphomas. Cancer. 1974;34:1851-1872.
13. Lamant L, Espinos E, Duplantier M, et al. Establishment of a novel anaplastic large-cell lymphoma-cell line (COST) from a "small-cell variant" of ALCL. Leukemia. 2004;18:1693-1698.
14. del Mistro A, Leszl A, Bertorelle R, et al. A CD30-positive T cell line established from an aggressive anaplastic large cell lymphoma, originally diagnosed as Hodgkin's disease. Leukemia. 1994;8:1214-1219.
15. Gentleman RC, Carey VJ, Bates DM, et al. Bioconductor: open software development for computational biology and bioinformatics. Genome Biol. 2004;5:R80.
16. Irizarry RA, Hobbs B, Collin F, et al. Exploration, normalization, and summaries of high density oligonucleotide array probe level data. Biostatistics. 2003;4:249-264.
17. Robinson D, Foulds L. Comparison of phylogenetic trees. Math Biosci. 1981;53:131-147.
18. Reiner A, Yekutieli D, Benjamini Y. Identifying differentially expressed genes using false discovery rate controlling procedures. Bioinformatics. 2003;19:368-375.
19. Al-Shahrour F, Diaz-Uriarte R, Dopazo J. FatiGO: a web tool for finding significant associations of Gene Ontology terms with groups of genes. Bioinformatics. 2004;20:578-580.
20. Liang Y, Zhou Y, Shen P. NF-κB and its regulation on the immune system. Cell Mol Immunol. 2004;1:343-350.
21. Alizadeh AA, Eisen MB, Davis RE, et al. Distinct types of diffuse large B-cell lymphoma identified by gene expression profiling. Nature. 2000;403:503-511.
22. Shipp MA, Ross KN, Tamayo P, et al. Diffuse large B-cell lymphoma outcome prediction by gene-expression profiling and supervised machine learning. Nat Med. 2002;8:68-74.
23. Rosenwald A, Wright G, Chan WC, et al. The use of molecular profiling to predict survival after chemotherapy for diffuse large-B-cell lymphoma. N Engl J Med. 2002;346:1937-1947.
24. Wright G, Tan B, Rosenwald A, Hurt EH, Wiestner A, Staudt LM. A gene expression-based method to diagnose clinically distinct subgroups of diffuse large B cell lymphoma. Proc Natl Acad Sci U S A. 2003;100:9991-9996.
25. Hoefnagel JJ, Dijkman R, Basso K, et al. Distinct types of primary cutaneous large B-cell lymphoma identified by gene expression profiling. Blood. 2005;105:3671-3678.
26. Rosenwald A, Wright G, Leroy K, et al. Molecular diagnosis of primary mediastinal B cell lymphoma identifies a clinically favorable subgroup of diffuse large B cell lymphoma related to Hodgkin lymphoma. J Exp Med. 2003;198:851-862.
27. Rosenwald A. DNA microarrays in lymphoid malignancies. Oncology (Williston Park). 2003;17:1743-1748; discussion 1750, 1755, 1758-1749 passim.
28. Klein U, Tu Y, Stolovitzky GA, et al. Gene expression profiling of B cell chronic lymphocytic leukemia reveals a homogeneous phenotype related to memory B cells. J Exp Med. 2001;194:1625-1638.
29. Basso K, Liso A, Tiacci E, et al. Gene expression profiling of hairy cell leukemia reveals a phenotype related to memory B cells with altered expression of chemokine and adhesion receptors. J Exp Med. 2004;199:59-68.
30. Dave SS, Wright G, Tan B, et al. Prediction of survival in follicular lymphoma based on molecular features of tumor-infiltrating immune cells. N Engl J Med. 2004;351:2159-2169.
31. Abraham RS, Ballman KV, Dispenzieri A, et al. Functional gene expression analysis of clonal plasma cells identifies a unique molecular profile for light chain amyloidosis. Blood. 2005;105:794-803.
32. Martinez-Delgado B, Melendez B, Cuadros M, et al. Expression profiling of T-cell lymphomas differentiates peripheral and lymphoblastic lymphomas and defines survival related genes. Clin Cancer Res. 2004;10:4971-4982.
33. Thompson MA, Stumph J, Henrickson SE, et al. Differential gene expression in anaplastic lymphoma kinase-positive and anaplastic lymphoma kinase-negative anaplastic large cell lymphomas. Hum Pathol. 2005;36:494-504.
34. Ballester B, Ramuz O, Gisselbrecht C, et al. Gene expression profiling identifies molecular subgroups among nodal peripheral T-cell lymphomas. Oncogene. 2006;25:1560-1570.
35. Martinez-Delgado B, Cuadros M, Honrado E, et al. Differential expression of NF-κB pathway genes among peripheral T-cell lymphomas. Leukemia. 2005;19:2254-2263.
36. Fillmore GC, Lin Z, Bohling SD, et al. Gene expression profiling of cell lines derived from T-cell malignancies. FEBS Lett. 2002;522:183-188.
37. Li S, Ross DT, Kadin ME, Brown PO, Wasik MA. Comparative genome-scale analysis of gene expression profiles in T cell lymphoma cells during malignant progression using a complementary DNA microarray. Am J Pathol. 2001;158:1231-1237.
38. Wellmann A, Thieblemont C, Pittaluga S, et al. Detection of differentially expressed genes in lymphomas using cDNA arrays: identification of clusterin as a new diagnostic marker for anaplastic large-cell lymphomas. Blood. 2000;96:398-404.
39. Carbone A, Gloghini A, Gaidano G, Dalla-Favera R, Falini B. BCL-6 protein expression in human peripheral T-cell neoplasms is restricted to $CD30^+$ anaplastic large-cell lymphomas. Blood. 1997;90:2445-2450.
40. Kerl K, Vonlanthen R, Nagy M, et al. Alterations on the 5' noncoding region of the *BCL-6* gene are not correlated with BCL-6 protein expression in T cell non-Hodgkin lymphomas. Lab Invest. 2001;81:1693-1702.
41. Ye BH, Lista F, Lo Coco F, et al. Alterations of a zinc finger-encoding gene, BCL-6, in diffuse large-cell lymphoma. Science. 1993;262:747-750.
42. Stein H, Mason DY, Gerdes J, et al. The expression of the Hodgkin's disease associated antigen Ki-1 in reactive and neoplastic lymphoid tissue: evidence that Reed-Sternberg cells and histiocytic malignancies are derived from activated lymphoid cells. Blood. 1985;66:848-858.
43. Chtanova T, Tangye SG, Newton R, et al. T follicular helper cells express a distinctive transcriptional profile, reflecting their role as non-Th1/Th2 effector cells that provide help for B cells. J Immunol. 2004;173:68-78.
44. Dupuis J, Boye K, Martin N, et al. Expression of CXCL13 by neoplastic cells in angioimmunoblastic T-cell lymphoma (AITL): a new diagnostic marker providing evidence that AITL derives from follicular helper T cells. Am J Surg Pathol. 2006;30:490-494.
45. Shaffer AL, Yu X, He Y, Boldrick J, Chan EP, Staudt LM. BCL-6 represses genes that function in lymphocyte differentiation, inflammation, and cell cycle control. Immunity. 2000;13:199-212.
46. Takekawa M, Itoh F, Hinoda Y, et al. Cloning and characterization of a human cDNA encoding a novel putative cytoplasmic protein-tyrosine-phosphatase. Biochem Biophys Res Commun. 1992;189:1223-1230.
47. Cong F, Spencer S, Cote JF, et al. Cytoskeletal protein PSTPIP1 directs the PEST-type protein tyrosine phosphatase to the c-Abl kinase to mediate Abl dephosphorylation. Mol Cell. 2000;6:1413-1423.

48. Honorat JF, Ragab A, Lamant L, Delsol G, Ragab-Thomas J. SHP1 tyrosine phosphatase negatively regulates NPM-ALK tyrosine kinase signaling. Blood. 2006;107:4130-4138.
49. Perlmutter DH, Cole FS, Kilbridge P, Rossing TH, Colten HR. Expression of the alpha 1-proteinase inhibitor gene in human monocytes and macrophages. Proc Natl Acad Sci U S A. 1985;82:795-799.
50. Isaacson P, Wright DH. Malignant histiocytosis of the intestine: its relationship to malabsorption and ulcerative jejunitis. Hum Pathol. 1978;9:661-677.
51. Isaacson PG, O'Connor NT, Spencer J, et al. Malignant histiocytosis of the intestine: a T-cell lymphoma. Lancet. 1985;2:688-691.
52. Villalva C, Trempat P, Greenland C, et al. Isolation of differentially expressed genes in NPM-ALK-positive anaplastic large cell lymphoma. Br J Haematol. 2002;118:791-798.
53. Chawla RK, Lawson DH, Sarma PR, Nixon DW, Travis J. Serum alpha-1 proteinase inhibitor in advanced cancer: mass variants and functionally inert forms. Cancer Res. 1987;47:1179-1184.
54. Harris CC, Primack A, Cohen MH. Elevated alpha1-antitrypsin serum levels in lung cancer patients. Cancer. 1974;34:280-281.
55. Laine A, Leroy A, Hachulla E, Davril M, Dessaint JP. Comparison of the effects of purified human alpha 1-antichymotrypsin and alpha 1-proteinase inhibitor on NK cytotoxicity: only alpha 1-proteinase inhibitor inhibits natural killing. Clin Chim Acta. 1990;190:163-173.
56. Lejeune PJ, Mallet B, Farnarier C, Kaplanski S. Changes in serum level and affinity for concanavalin A of human alpha 1-proteinase inhibitor in severe burn patients: relationship to natural killer cell activity. Biochim Biophys Acta. 1989; 990:122-127.
57. Okumura Y, Kudo J, Ikuta T, Kurokawa S, Ishibashi H, Okubo H. Influence of acute-phase proteins on the activity of natural killer cells. Inflammation. 1985;9:211-219.
58. Jundt F, Raetzel N, Muller C, et al. A rapamycin derivative (everolimus) controls proliferation through down-regulation of truncated CCAAT enhancer binding protein β and NF-κB activity in Hodgkin and anaplastic large cell lymphomas. Blood. 2005;106:1801-1807.
59. McKnight SL. McBindall—a better name for CCAAT/enhancer binding proteins? Cell. 2001; 107:259-261.
60. Ramji DP, Foka P. CCAAT/enhancer-binding proteins: structure, function and regulation. Biochem J. 2002;365:561-575.
61. Brembeck FH, Rosario M, Birchmeier W. Balancing cell adhesion and Wnt signaling, the key role of beta-catenin. Curr Opin Genet Dev. 2006;16: 51-59.
62. Chen RH, McCormick F. Selective targeting to the hyperactive beta-catenin/T-cell factor pathway in colon cancer cells. Cancer Res. 2001;61:4445-4449.
63. Chen S, Guttridge DC, You Z, et al. Wnt-1 signaling inhibits apoptosis by activating beta-catenin/T cell factor-mediated transcription. J Cell Biol. 2001;152:87-96.
64. Esufali S, Bapat B. Cross-talk between Rac1 GTPase and dysregulated Wnt signaling pathway leads to cellular redistribution of beta-catenin and TCF/LEF-mediated transcriptional activation. Oncogene. 2004;23:8260-8271.
65. Barker N, Morin PJ, Clevers H. The yin-yang of TCF/beta-catenin signaling. Adv Cancer Res. 2000;77:1-24.
66. Kikuchi A. Regulation of beta-catenin signaling in the Wnt pathway. Biochem Biophys Res Commun. 2000;268:243-248.